REPORT DOCUMENTATION PAGE

Form Approved
OMB No. 0704-0188

1. REPORT DATE *(DD-MM-YYYY)*	2. REPORT TYPE	3. DATES COVERED *(From - To)*
	Technical Papers	

4. TITLE AND SUBTITLE

5a. CONTRACT NUMBER

5b. GRANT NUMBER

5c. PROGRAM ELEMENT NUMBER

6. AUTHOR(S)

5d. PROJECT NUMBER

5e. TASK NUMBER

5f. WORK UNIT NUMBER

7. PERFORMING ORGANIZATION NAME(S) AND ADDRESS(ES)

Air Force Research Laboratory (AFMC)
AFRL/PRS
5 Pollux Drive
Edwards AFB CA 93524-7048

8. PERFORMING ORGANIZATION REPORT

9. SPONSORING / MONITORING AGENCY NAME(S) AND ADDRESS(ES)

Air Force Research Laboratory (AFMC)
AFRL/PRS
5 Pollux Drive
Edwards AFB CA 93524-7048

10. SPONSOR/MONITOR'S ACRONYM(S)

11. SPONSOR/MONITOR'S NUMBER(S)

12. DISTRIBUTION / AVAILABILITY STATEMENT

Approved for public release; distribution unlimited.

13. SUPPLEMENTARY NOTES

14. ABSTRACT

15. SUBJECT TERMS

16. SECURITY CLASSIFICATION OF:			17. LIMITATION OF ABSTRACT	18. NUMBER OF PAGES	19a. NAME OF RESPONSIBLE PERSON
a. REPORT	b. ABSTRACT	c. THIS PAGE			Leilani Richardson
Unclassified	Unclassified	Unclassified	A		19b. TELEPHONE NUMBER *(include area code)* (661) 275-5015

41 items enclosed

MEMORANDUM FOR PRS (In-House Publication)

11 Jan 2001

FROM: PROI (STINFO)

SUBJECT: Authorization for Release of Technical Information, Control Number: **AFRL-PR-ED-TP-2001-010**
Bromaghim, D.R., et. al., "Radiometric Analysis From the 26kW Electric Propulsion Space Experiment (ESEX) Flight"

(Statement A)

Paper for the Journal of Propulsion and Power
(Deadline: N/A)

Radiometric Analysis from the 26-kW Electric Propulsion Space Experiment (ESEX) Flight

G.G. Spanjers*, J.H. Schilling†, D.R. Bromaghim‡

Propulsion Directorate, AFRL/PRSS, Air Force Research Laboratory, Edwards AFB, CA 93524

L.K. Johnson§, The Aerospace Corporation, 2350 E. El Segundo Blvd., El Segundo, CA 90245

Abstract

The United States Air Force Research Laboratory's Electric Propulsion Space Experiment (ESEX) was launched and operated in early 1999 in order to demonstrate the compatibility and readiness of a 30-kW class ammonia arcjet for satellite propulsion applications. As part of this flight, an array of on-board contamination sensors was used to assess the effect of the arcjet and other environments on the spacecraft. The sensors consisted of microbalances to measure material deposition, radiometers to assess material degradation due to thermal radiation, and solar cell segments to investigate solar array degradation. Over eight firings of the ESEX arcjet, and 33 minutes, 26 seconds operating time, the radiometer near the thruster, viewing the arcjet plume and body, experiences a change in the thermal properties of its coating ~~from the firings~~ (repetitive). Radiometers with no view of the arcjet, or a view of only the plume, show no change. In general, contamination effects are observed only on sensors near the thruster exhaust nozzle, a location unlikely to be used in an operational high-power electric propulsion system. No contamination effects are observed in the backplane of the thruster. For future programs, while engineering measures may be needed for spacecraft equipment in the immediate vicinity of the thruster body, the arcjet environment is generally benign.

---

* Project Scientist, Member AIAA

† Project Engineer, Sparta Inc., Air Force Research Laboratory, Edwards AFB, CA, Member AIAA; Present address: W.E. Research, 4360 San Juan Court, Rosamond, CA 93560

‡ ESEX Program Manager, Member AIAA

§ ESEX Chief Scientist, Present address: Jet Propulsion Laboratory, MS 125-109, 4800 Oak Grove Dr., Pasadena, CA 91109

Nomenclature

$A =$	**Area**
$C_P =$	**Specific Heat**
$Q_{IN} =$	**Heat flux into sensor**
$Q_{RAD} =$	**Radiative heat flux**
$Q_T =$	**Heat flux conducted down radiometer stem**
$Q_{12} =$	**Radiative heat within radiometer body**
$T =$	**Temperature**
$k =$	**Thermal Conductivity**
$m =$	**mass**

Suggest unbolding definitions

- watch spacing for consistency w/ other headings

I. Introduction

Spacecraft ~~thermal control~~ surfaces can be degraded by excessive heat flux, which can alter the emissive and absorptive properties of spacecraft materials, changing the thermal balance of the satellite. Understanding the coupling of these effects with high-power electric propulsion is of critical importance to the development of the next-generation of large United States Air Force (USAF) space structures. A major goal of the USAF Electric Propulsion Space Experiment (ESEX)[1] is to explore these issues by measuring the contamination effects of a 30-kW class arcjet in flight. ESEX was launched on 23 February 1999 as 1 of 9 experiments aboard the USAF's Advanced Research and Global Observation Satellite (ARGOS)[2].

Suggest spelling out

An array of sensors is positioned at strategic locations of the ESEX package in order to assess the contamination effects. ~~Thermal~~ surface degradation due to the arcjet firing is measured using four radiometers. These radiometers are coated with S13-GLO white paint, a ~~common thermal~~ ~~surface~~ material with low solar absorptivity and high emissivity. Measurement of heat transfer through the coating determines the degradation of S13-GLO when subjected to the spectral emission of the high-power arcjet. This degradation impacts the thermal design of spacecraft using high-power electric propulsion. Mass deposition is measured using four thermoelectric quartz crystal microbalances (TQCMs).[3] A sample Gallium Arsenide (GaAs) solar array segment placed near the arcjet nozzle determines impact on the satellite power generation capability.[4] Electromagnetic interference is characterized using a set of on-board antennas and ground stations.[5] This paper focuses on heat flux and material degradation measurements from the radiometers. Measurements from the other on-board sensors can be found in companion papers within this issue.

During ~~8~~ eight firings of the ESEX arcjet, the radiometer placed near the thruster exit, with a view of both the arcjet plume and body, shows material degradation of the sensor ~~thermal~~ coating ~~from the arcjet firings~~. Radiometers with no view of the arcjet, or a view of only the plume, show no measurable degradation. Although degradation associated with contamination ~~is~~ was observed, the effect ~~is~~ was observed only on sensors placed very near, and with a direct view, of the exhaust nozzle of the thruster. It is highly unlikely that material or sensors would be located this close to the thrusters exit plane in an operational high-power electric-propulsion system. Contamination sensors located in the backplane of the arcjet show no deleterious effects. For future programs, while engineering measures may be needed for spacecraft equipment in the immediate vicinity of the thruster body, the arcjet environment is generally benign.

II. On-Board Radiometer Sensors

The ESEX flight unit is equipped with four microbalances, four radiometers, and two sections of GaAs solar array cells. The sensors are positioned on the ESEX flight unit as shown in Fig. 1. Specific radiometer sensor locations are listed in Table 1. In Table 1, angle=0 is defined as horizontal to the thruster exit plane with negative values in the backflow region; and when sensor angle=90 if the sensor normal is directed towards the thruster exit.

The locations of the ESEX radiometers relative to the arcjet nozzle are shown in Fig. 2. Radiometer #1 is located on the diagnostic tower adjacent to TQCM #1, where it has a direct view of the arcjet body and plume. Radiometers #2 and #4 have a view of the arcjet plume, but are blocked from arcjet body emission by the thermal shield. Radiometer #3 on the diagnostic deck has no direct view of either the arcjet body or plume.

These sensors, shown schematically in Fig. 3, consist of titanium witness plates supported by a narrow titanium strut and an insulating nylon bushing. A reflective aluminum housing surrounds the entire assembly except for an aperture on the front face. The temperature of the radiometer sensor and base are measured using thermocouples with an accuracy of ±1°C. The temperature measurements are used to calculate the heat flux through the radiometer assembly according to:

$$Q_{IN} = Q_{RAD} + Q_{12} + kA\frac{dT}{dx} + mC_P\frac{dT}{dt}$$

The Q_{12} and, in equilibrium, $mC_P\ dT/dt$ terms are negligible. Thus, the temperature difference across the stem corresponds to the net radiative heat flux from the sensor head. This is dominated by infrared (IR) graybody emissivity (Q_{RAD}) and, when in sunlight, solar absorbtivity (Q_{IN}). Thus the eclipse or shadow temperature difference between sensor head and base corresponds directly to the IR emissivity of the face, and with this emissivity known measurements in sunlight can be

used to determine solar absorptivity. The time response of the radiometer, due to the thermal inertia of the sensor head, is approximately fifteen minutes.

The radiometer face is coated with S13-GLO white paint with a nominal emissivity of approximately 0.25 in the visible range, increasing to 0.85 in the infrared. This is a commonly used coating for spacecraft thermal control, but is known to degrade due to solar UV and charged particle interactions, with changes in emissivity and absorptivity. The degradation of the coating in response to the emission spectrum of the arcjet is not known but will be explored as part of the ESEX flight experiment.

III. Flight Data

The ARGOS host spacecraft for ESEX was launched 23 February 1999 from Vandenberg AFB using a Delta II launcher into a 97-degree, near-polar orbit at 846-km altitude. The ESEX contamination diagnostics were powered up to receive data 1 hour, 25 minutes after launch. A total of eight ESEX firings were performed between 15 March 1999 and 21 April 1999. Following the eight firings a battery anomaly occurred which precluded additional firings. The ESEX events, including the battery anomaly, are described in detail in Ref. 1. A summary of the ESEX events related to the contamination measurements is shown in Table 2.

Figures 5 and 6 shows the sensor and base temperatures for radiometer #1 during the period surrounding Firing #4. At eight minutes, Firing #4 was the longest of the ESEX experiment. Figure 5 shows the radiometer temperatures oscillating with the solar cycle as ARGOS orbits. Figure 6 shows the same data on an expanded time base to illustrate the details of the radiometer response to the arcjet firing. Both the base and sensor temperatures are observed to rise through the firing, never achieving a thermal equilibrium. Other observations, particularly video images[6] and solar cell measurements, indicate that radiant emissions from the arcjet remain nearly

constant after the first two or three minutes of operation. In addition, the arcjet itself nearly reaches thermal equilibrium in that period.[7]

However, the radiometers do maintain near-equilibrium conditions during the much slower variations in solar illumination during the ARGOS orbit period. This allows us to determine the heat absorbed by the radiometers over the course of the solar cycle. Since solar illumination as a function of orbit phase is known and repeatable, this will serve as an indirect measurement of the solar absorbtivity and infrared emissivity of the radiometer surface coating. As seen in figure 5, the behavior of the radiometers over the solar cycle is very consistently repeatable before the arcjet firing. After the arcjet firing, the long-term behavior is again consistently repeatable, but the average temperature of the sensor head and base has increased by several degrees. The temperature difference between the two during periods of illumination has similarly increased, while the temperature difference in shadow remains approximately constant.

Figure 7 shows the behavior of the radiometers throughout the mission, with the arcjet firings indicated for reference. The heat flux calculated from radiometer sensor head and base temperatures are plotted at the point of maximum incident solar flux during the orbit period, corresponding quite closely to the maximum observed heat flux in the radiometers – as expected for a system at or close to thermal equilibrium. Again, we see a secular increase associated with the arcjet firings.

Radiometer #1, with close, direct exposure to the arcjet plume and body, shows the most dramatic effect. Prior to the arcjet firings, radiometer #1 measures a fairly constant 0.27 W heat load at the peak of the solar cycle. With the onset of arcjet activity, this value shows a steady rise, reaching a value of 0.36 W after seven arcjet firings totaling 33 minutes of operation. This suggests a

corresponding increase in the solar absorbtivity of the surface coating of the radiometer. Another, smaller increase, to 0.39 W, is observed following the battery anomaly on Day 114..

Radiometers #2 and #4 exhibit similar behavior, but to a much smaller degree. As these radiometers are shielded from arcjet body radiation, and see the plume from a greater distance than does radiometer #1, this is unsurprising. Radiometer #3, completely shielded from the arcjet, shows no significant change in heat flux or surface properties. None of the radiometers show any noticeable change in heat flux during the eclipsed portion of the orbit, suggesting that the infrared emissivity of the surface coating does not change.

IV. Discussion

The rise in sensor head temperature during arcjet firing indicates that the radiometer is receiving a substantial radiated heat load from the arcjet. However, as the radiometers do not reach thermal equilibrium during a single arcjet firing, any attempt to quantify this heat load would require a detailed transient model of the radiometers. Since there is substantial uncertainty regarding key parameters for such a model, such as the heat capacities of the internal components of the sensor, such an analysis cannot be presented in this paper. The radiated heat of an operating arcjet is in any event dominated by blackbody emission from the body surface, which can be readily measured in ground experiments.

The secular changes in radiometer behavior, especially that of radiometer #1, suggest a permanent change in the surface properties of the S13-GLO coating as a result of exposure to arcjet plume and body radiation. The observed heat flux during periods when the radiometers are in shadow does not change. As radiometer behavior in shadow is dominated by IR emission, we conclude that the IR emissivity of the S13-GLO coating is not significantly changed. However, the ~30% increase in heat flux at maximum solar illumination is significant and suggests a

similar increase in the solar absorptivity of the surface. This is consistent with the white paint charring or otherwise darkening due to the estimated 1 watt/cm^2 radiation flux from the arcjet body. Radiometers shielded from this effect exhibit much smaller changes in absorbtivity.

spacing

V. Summary and Conclusions

A preliminary analysis of the data from the ESEX flight is performed to assess the contamination associated with the use of the 30-kW arcjet. Radiometer data indicates material degradation of the S13-GLO coating only for the radiometer nearest the arcjet nozzle with a full view of the exhaust plume and the arcjet body. A 30% increase in heat transfer through the coating is observed following the ~~8~~ eight arcjet firings. Radiometers obscured from the arcjet body, with a view of only the plume, showed no evidence of surface coating degradation. Due to a lack of thermal equilibrium during the arcjet firings, further transient analysis of radiometers is required to assess the heat flux due to the arcjet firings.

In general, deleterious contamination effects were observed only for sensors placed very near the arcjet nozzle – much closer than would be designed on an operational spacecraft. Sensors showed no contamination effects in the thruster backplane. The ESEX data suggests that the contamination associated with the operation of high-power electric propulsion can be controlled through relatively simple design adjustments.

spacing

VI. Acknowledgements

The authors would like to extend their gratitude for the expert technical contributions of Mary Kriebel, Don Baxter, Bob Tobias, David Lee, David Huang, and N. John Stevens of TRW in the design and development of the flight diagnostic package. We also acknowledge the ARGOS program office and the flight operations team at Kirtland AFB for their technical expertise, as well as their insight and flexibility in the mission operations.

Do these need to be capitalized?

spacing

VII. References

[1] D.R. Bromaghim, et al., "An Overview of the On-Orbit Results from the ESEX Flight Experiment," AIAA paper 99-2706, June 1999. Also submitted to this issue, J. Prop and Power.

[2] B.J. Turner, and F.J. Agardy, "The Advanced Research and Global Observation Satellite (ARGOS) Program," AIAA paper 94-4580, Sept. 1994.

[3] Spanjers, G. G., Schilling, J. H., Bromaghim, D. B., Johnson, L. K., "Mass Deposition Measurements from the ESEX 26 kW Ammonia Arcjet Flight Experiment," submitted to this issue, Journal of Propulsion and Power.

[4] Schilling, J. H., Spanjers, G. G., Bromaghim, D. B., Johnson, L. K., "Solar Cell Degradation during the ESEX 26 kW Ammonia Arcjet Flight Experiment," submitted to this issue, Journal of Propulsion and Power.

[5] Dulligan, M. J., Bromaghim, D. B., Zimmerman, J. A., Hardesty, D., Johnson, L. K., "Observations of the Effect on Spacecraft Function and Communications by the ESEX 26kW Ammonia Arcjet Operation," submitted to this issue, Journal of Propulsion and Power.

[6] L.K. Johnson et al., "Optical Diagnostics Applied to the Air Force Electric Propulsion Space Experiment (ESEX)," submitted to this issue, Journal of Propulsion and Power.

[7] J.M. Fife, et al. "Orbital Performance Analysis of the Air Force Electric Propulsion Space Experiment (ESEX)," submitted to this issue, Journal of Propulsion and Power.

Last name first

Please spell out to be consistent w/ other references

Last name first

Table 1: Locations of Radiometer Sensors Relative to Arcjet Exhaust Plane

	Distance (cm)	Angle (degrees)	Sensor Angle (degrees)
Radiometer #1	40	-11	79
Radiometer #2	48	-37	53
Radiometer #3	45	-60	60
Radiometer #4	60	-41	41

Table 2: Contamination Events during ESEX Flight Experiment

Firing (F) or Event	Date/Time (Zulu)	Julian Date	Duration
Boom Deployed	09MAR99 14:59:57	68.62497	
F-1C	15MAR99 21:55:55	74.91383	2 m, 21 s
F-2	19MAR99 22:32:23	78.93916	5 m, 1 s
F-3	21MAR99 12:24:41	80.51714	5 m, 33 s
F-4	23MAR99 21:27:57	82.89441	8 m, 2 s
F-5	26MAR99 12:45:25	85.53154	6 m, 4 s
F-6	31MAR99 13:05:37	90.54557	4 m, 29 s
F-7	02APR99 22:09:03	92.92295	53 s 38 s
F-8	21APR99 12:22:12	111.51542	42 s
Battery Anomaly	22APR99 15:18:37	112.63793	

Figure Captions:

Fig. 1 (a) Top view and (b) Side view of ESEX showing the locations of the contamination sensors.

Fig. 2 Locations of the four Radiometers relative to the arcjet nozzle.

Fig. 3 Schematic diagram of the ESEX Radiometers. The radiometer base is 2.9 inches in diameter.

Fig. 4 Radiometer behavior over several orbit periods

Fig. 5 Radiometer behavior during arcjet firing.

Fig. 6 Radiometer peak heat flux. Vertical lines denote times of eight arcjet firings.

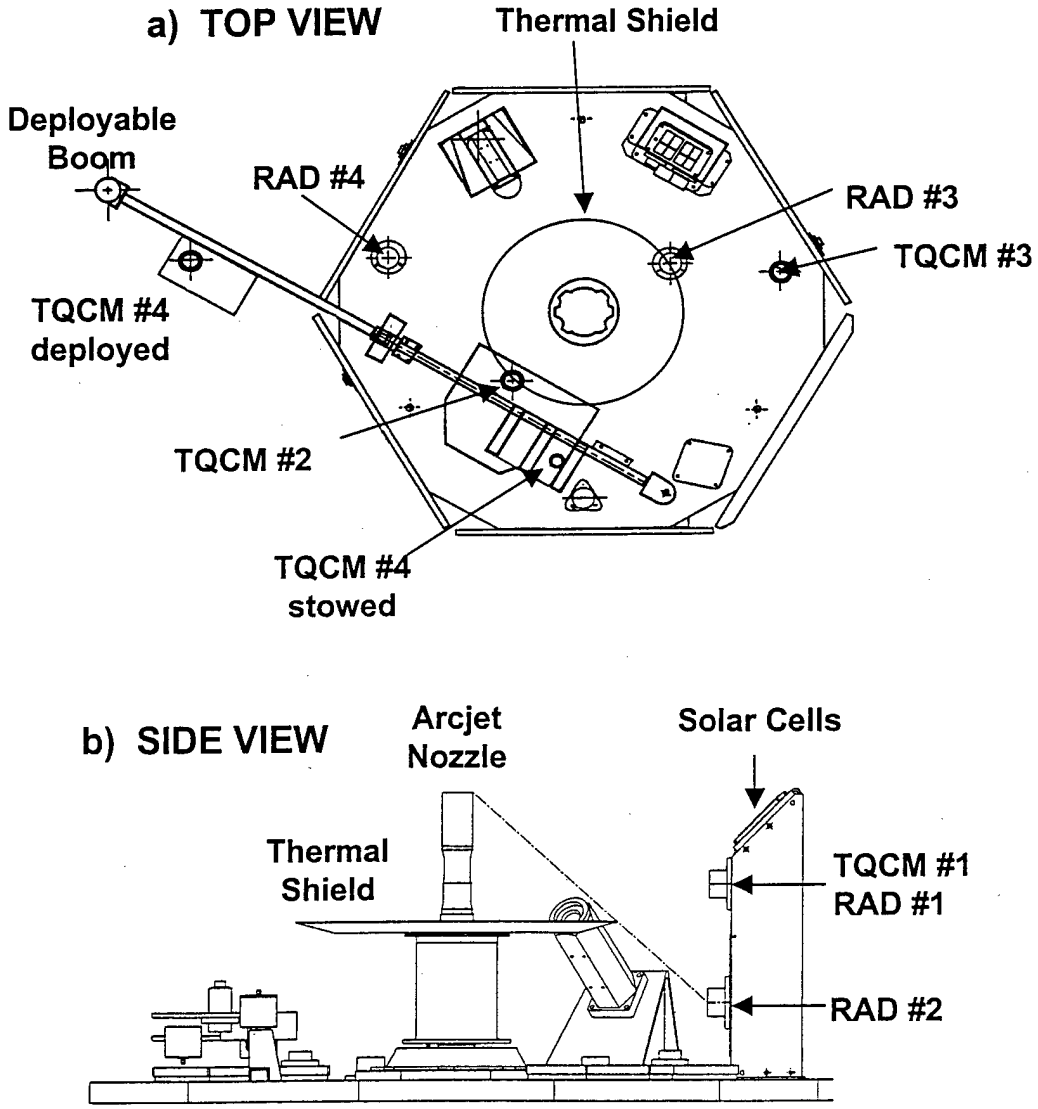

Spanjers et al., J. Prop and Power, Fig. 1 of 6

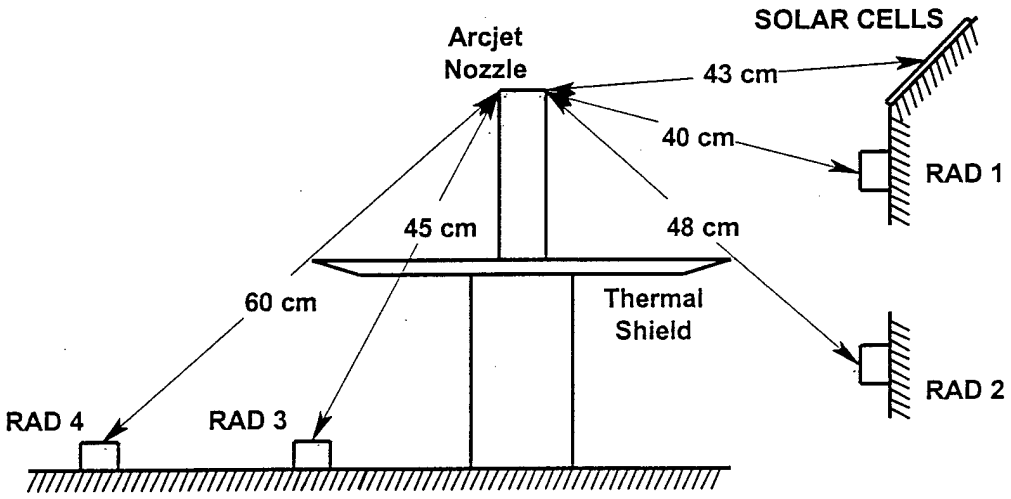

Spanjers et al., J. Prop and Power, Fig. 2 of 6

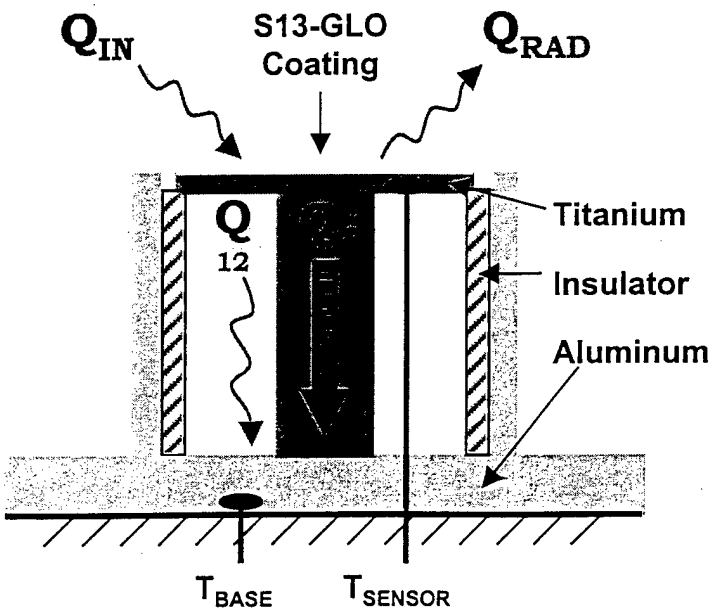

Spanjers et al., J. Prop and Power, Fig. 3 of 6

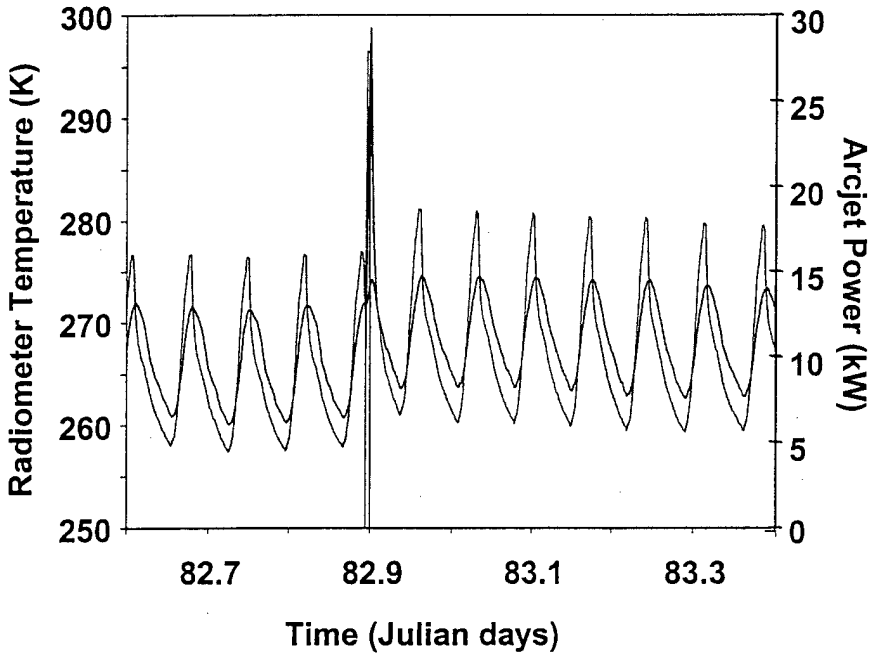
Radiometer Temperature (K)
300
290
280
270
260
250
Arcjet Power (kW)
30
25
20
15
10
5
0
82.7
82.9
83.1
83.3
Time (Julian days)

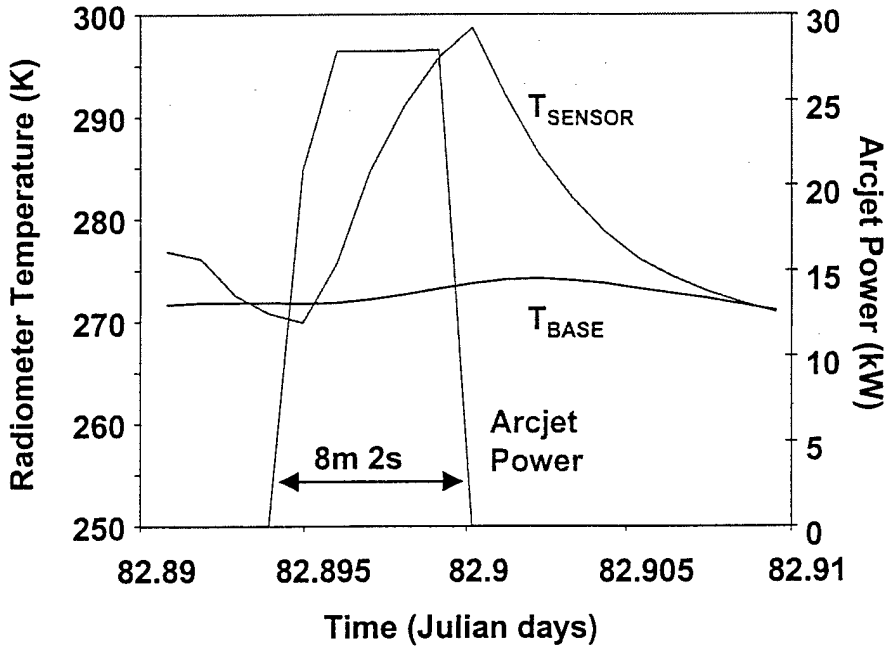

Spanjers et al., J. Prop and Power, Fig. 5 of 6

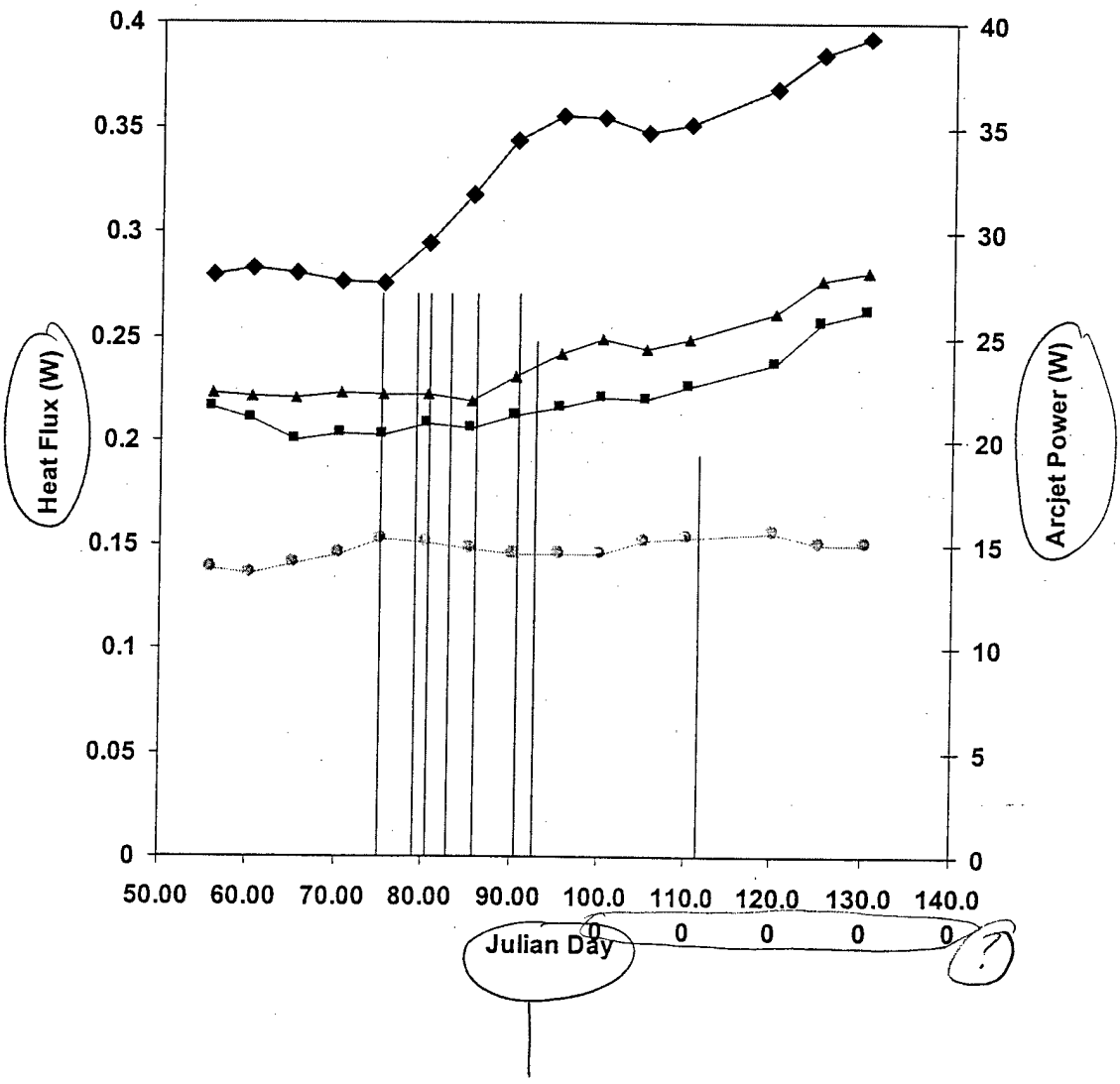

Please make axis label font same size as those in preceeding figures

Spanjers et al., J. Prop and Power, Fig. 6 of 6